Mechanical detection of electron spin resonance beyond 1 THz

Takahashi, Hideyuki

Ohmichi, Eiji

Ohta, Hitoshi

(Citation)
Applied Physics Letters,107(18):182405-182405

(Issue Date)
2015-11-02

(Resource Type)
journal article

(Version)
Version of Record

Mechanical detection of electron spin resonance beyond 1 THz

Hideyuki Takahashi, Eiji Ohmichi, and Hitoshi Ohta

Citation: Applied Physics Letters **107**, 182405 (2015); doi: 10.1063/1.4935204
View online: http://dx.doi.org/10.1063/1.4935204
View Table of Contents: http://scitation.aip.org/content/aip/journal/apl/107/18?ver=pdfcov
Published by the AIP Publishing

Mechanical detection of electron spin resonance beyond 1 THz

Hideyuki Takahashi,[1] Eiji Ohmichi,[2] and Hitoshi Ohta[3]
[1]*Organization of Advanced Science and Technology, Kobe University, 1-1, Rokkodai, Nada, Kobe 657-8501, Japan*
[2]*Graduate School of Science, Kobe University, 1-1 Rokkodai-cho, Nada, Kobe 657-8501, Japan*
[3]*Molecular Photoscience Research Center, Kobe University, 1-1 Rokkodai-cho, Nada, Kobe 657-8501, Japan*

(Received 27 August 2015; accepted 22 October 2015; published online 3 November 2015)

We report the cantilever detection of electron spin resonance (ESR) in the terahertz (THz) region. This technique mechanically detects ESR as a change in magnetic torque that acts on the cantilever. The ESR absorption of a tiny single crystal of Co Tutton salt, $Co(NH_4)_2(SO_4)_2{\cdot}6H_2O$, was observed in frequencies of up to 1.1 THz using a backward travelling wave oscillator as a THz-wave source. This is the highest frequency of mechanical detection of ESR till date. The spectral resolution was evaluated with the ratio of the peak separation to the sum of the half-width at half maximum of two absorption peaks. The highest resolution value of 8.59 ± 0.53 was achieved at 685 GHz, while 2.47 ± 0.01 at 80 GHz. This technique will not only broaden the scope of ESR spectroscopy application but also lead to high-spectral-resolution ESR imaging. © *2015 AIP Publishing LLC*.
[http://dx.doi.org/10.1063/1.4935204]

Magnetic resonance spectroscopy is a widely employed technique in physics, chemistry, biology, medicine, and materials science. It provides structural and dynamical information of samples via their nuclear and electron spins. Since the spectral resolution and signal intensity increase with the external field, it is important to extend this technique to a higher field and frequency range. In fact, the development of 1 GHz nuclear magnetic resonance technique, which has been a hot issue in recent years, enables precise structural analysis of massive molecules such as proteins.[1] Also, in electron spin resonance (ESR), the extension to higher frequency range is strongly desirable to broaden its range of applications. Many phenomena cannot be investigated by commercially available spectrometers that operate between the X- and W-bands (10–90 GHz). The examples include field-induced phase transitions, magnetic materials with broad line widths, and metal proteins with large zero-field splitting.[2]

ESR spectroscopy is conventionally performed with either the cavity perturbation method[3] or the transmission method.[4] Although the former method has been well established between the X- and W-bands, the cavity dimensions become too small to handle as the frequency increases. The latter method is easily extended above 100 GHz. However, the sensitivity is not very high; therefore, a large sample mass (typically, ∼mg) is required. The lack of a high-power light source also makes these methods difficult above 300 GHz. Several alternative methods for the high-frequency region have been proposed that are based on detection of the magnetization change accompanied by ESR. The examples include techniques that use a Hall sensor,[5] a SQUID magnetometer,[6–8] and a micro-cantilever.[9–11] The mechanical detection method using the micro-cantilever is particularly promising. The spin sensitivity is 3–6 orders of magnitude better than the transmission technique. The simple experimental setup enables a variety of applications, such as angle-dependent measurement and pulsed magnetic field measurement.[12,13] The same principle is also used in magnetic resonance force microscopy (MRFM).[14] Therefore, extending this technique to higher frequencies directly leads to MRFM imaging with high spectral resolution as well. In this letter, we report the mechanically detected ESR up to 1.1 THz, which is three times higher than the highest reported frequency till date.[15]

The experimental setup of cantilever-detected ESR spectroscopy is shown in Fig. 1. We used a commercial self-sensing silicon microcantilever, PRC-400 (Hitachi High-Technologies Corp.) with a spring constant $k = 2$–$3\,\mathrm{N/m}$ and dimensions of $400 \times 50 \times 5\,\mu\mathrm{m}^3$.[16] The cantilever was ion implanted with boron to make a piezoresistive path at the cantilever legs. The short reference lever fabricated on the same substrate cancels out the thermal drift and magnetoresistance. The unloaded cantilever has a eigenfrequency of $f_0 = 35 - 40\,\mathrm{kHz}$. When the magnetic field is applied to the magnetically anisotropic sample on the cantilever, the magnetic torque, $\boldsymbol{\tau} = \boldsymbol{M} \times \boldsymbol{H}$, causes the deflection of the cantilever. This deflection is detected as the change in resistance in the piezoresistive layer using the Wheatstone bridge circuit. Note that the torque detection method is not applicable to magnetically isotropic samples. The use of magnetic field gradient force is valid in these cases.[17]

Gunn oscillators below 160 GHz and backward traveling wave oscillators (BWO) above 217 GHz were used as the light source. By adjusting the cathode voltage of the BWO tube, the quasi-continuous electromagnetic waves were generated. This study used a series of BWO, OV-30, 32, 81, and 83 that spanned a frequency range of 217–1154 GHz. Since the BWO contained permanent magnets, it was located 1.5 m away from a 15 T superconducting magnet to avoid the influence of a stray magnetic field. A mechanical chopper for lock-in detection modulated the emitted electromagnetic wave. It then propagated through an oversized circular waveguide to the sample space inside the superconducting magnet. At the bottom of the waveguide, a brass horn was used to focus the electromagnetic wave onto a sample-mounted cantilever. The BWOs have a nominal output power of 1–10 mW. However, the electromagnetic wave is significantly

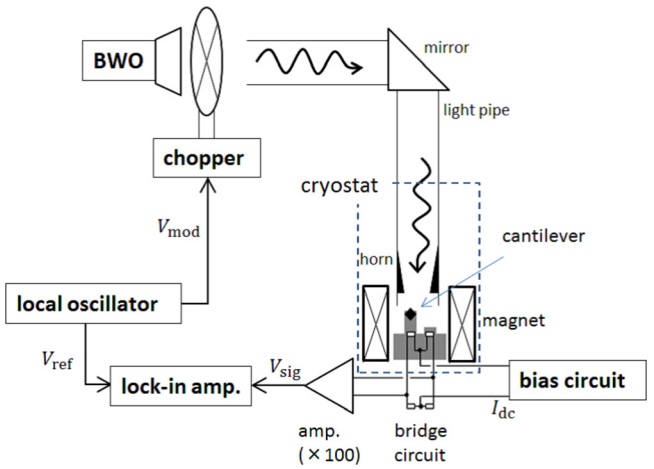

FIG. 1. Schematic of the cantilever-detected ESR measurement system using BWO.

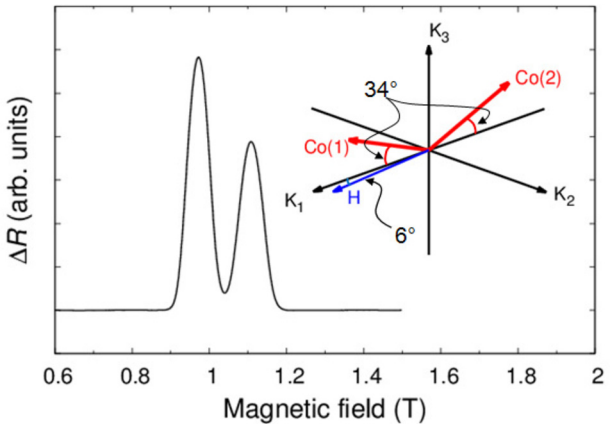

FIG. 2. ESR spectrum of Co Tutton salt at 80 GHz. ΔR denotes the change in the resistance of the piezoresistive layer on the cantilever from the off-resonant condition. The inset shows the symmetry axes of the inequivalent Co^{2+} ions (red) and the magnetic field direction (blue) with the orthogonal K_1, K_2, and K_3 axes. The symmetry axes are in the K_1-K_3 plane.

attenuated inside the waveguide. Moreover, the dimension of the concentrating horn outlet (3 mm diameter) is much larger than that of the cantilever. Therefore, the actual power irradiated on the sample is at most on the order of μW.

The sample is a single crystal of Co Tutton salt, $Co(NH_4)_2(SO_4)_2{\cdot}6H_2O$. The unit cell has two inequivalent Co^{2+} ions surrounded by six water molecules in a uniaxially distorted octahedral environment. This sample was determined to be suitable for the testing sample of torque-detected ESR because of its high spin density and large magnetic anisotropy. After a small crystal ($230 \times 200 \times 40\,\mu m^3$) was mounted on the cantilever using small amount of araldite epoxy glue, its eigenfrequency decreased to $f = 2.5$ kHz. The sample mass m was estimated to be approximately 4 μg by the equation: $m = (k/4\pi^2)(f^{-2} - f_0^{-2})$. This value contrasts the 1–10 mg sample mass usually required by conventional high-frequency ESR measurement with the transmission method. The sample was placed in a helium gas atmosphere ($P \sim 0.1$ atm) to ensure thermal equilibrium. The sample temperature was maintained at 4.2 K in all the measurements.

Figure 2 shows the ESR spectrum at 80 GHz obtained in the swept magnetic field. The magnetization of the sample periodically changed at the modulation frequency and was detected by the lock-in amplifier at the resonant field. Two individual absorption lines derived from inequivalent Co^{2+} ions are observed in accordance with the previous reports.[18]

The higher and lower resonant fields (H_1 and H_2) correspond to $g = 5.37 \pm 0.02$ and 5.96 ± 0.01, respectively.

Defining the orthogonal axes (K_1, K_2, and K_3) helps to analyze the ESR spectrum of Co Tutton salt (see the inset of Fig. 2). The K_3 axis is a bisector of the symmetry axes of two inequivalent Co^{2+} ions. The symmetry axes are in the K_1–K_3 plane and have a 34° angle with the K_1 axis. For the paramagnet with axial symmetry, the g-factor depends on the angle between the symmetry axis and the field direction θ as

$$g(\theta) = \sqrt{g_{\parallel}^2 \cos^2\theta + g_{\perp}^2 \sin^2\theta}, \quad (1)$$

where $g_{\parallel} = 6.5$ and $g_{\perp} = 3.1$ are the values when the field is applied parallel and perpendicular to the symmetry axis, respectively.[18] From this equation, we can deduce that the magnetic field direction is nearly in the K_1–K_3 plane and slightly tilted from the K_1 axis at a $6 \pm 2°$ angle.

The spectral resolution is quantitatively evaluated with the ratio of peak separation $h = H_1 - H_2$ to the sum of the half-width at half maximum of two peaks $w = W_1 + W_2$. From the fittings by Gaussian functions, we obtained $h/w = 2.47 \pm 0.01$ at 80 GHz.

Figure 3 shows the ESR spectra obtained between 290 GHz and 1.1 THz using the BWO. Although the signal-to-noise ratio (S/N) decreases at higher frequency where the

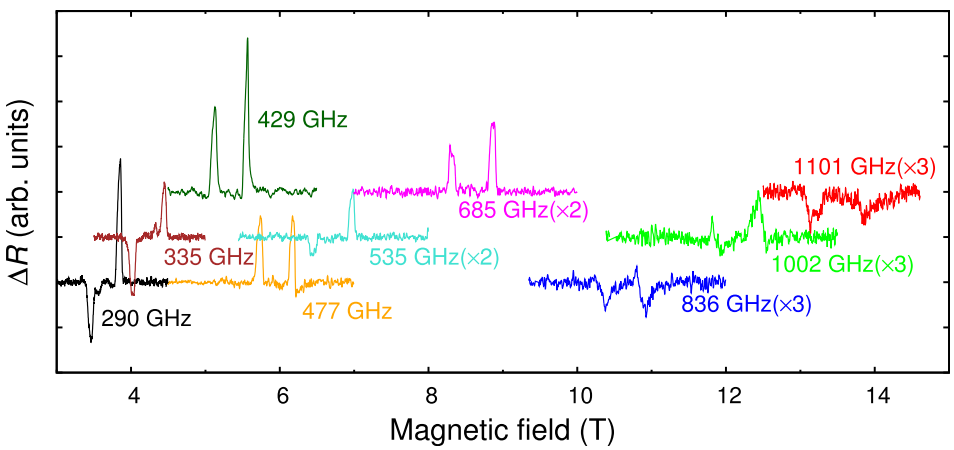

FIG. 3. ESR spectra of Co Tutton salt between 290 GHz and 1.1 THz obtained using BWO. The data are vertically shifted for clarity after the smooth background was subtracted. The data above 535 GHz are magnified.

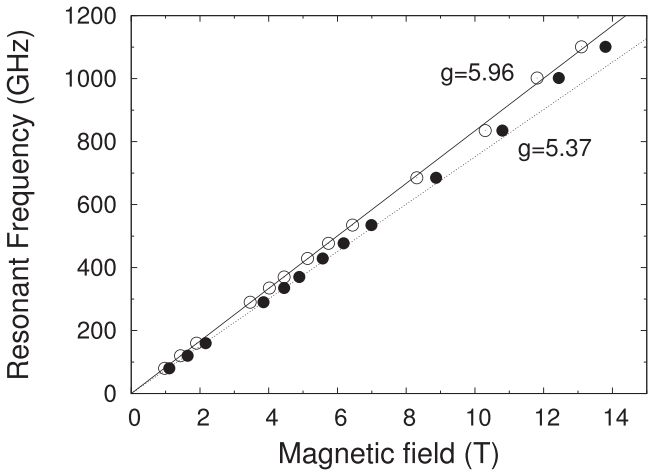

FIG. 4. The frequency-magnetic field diagram of ESR. The open (closed) dots correspond to the lower (higher) peaks of ESR spectra. The straight lines show the paramagnetic lines with corresponding g-factors.

BWO output becomes lower, the resonant peaks were observed at all frequencies. The modulation frequency was tuned to the eigenfrequency of the cantilever in these measurements to enable maximum sensitivity. However, we have to be careful that the cantilever oscillation is induced not only by the periodical change of $\boldsymbol{M}$ but also by the photothermal effect. The photothermal oscillation influence has two characteristics. The first is the offset of the lock-in amplitude signal. The large offset was especially observed when the modulation frequency coincided with the eigenfrequency of the cantilever. Fortunately, the photothermally induced offset has flat field dependence and does not obscure the ESR signals. The second characteristic is the inverse polarity of the ESR signal. The phases of the photothermal oscillation and periodical change in τ differ. Therefore, the amplitude of the cantilever reduces to less than that of the off-resonant condition when the two oscillations are out of phase. This results in the negative polarity of the ESR signal.

Figure 4 shows the frequency-magnetic field diagram of the ESR absorption peaks. The data are reasonably fitted by the straight line with a slope that corresponds to $g = 5.37$ and 5.96 at lower fields. As also shown in Fig. 3, two peaks that slightly overlapped at 80 GHz clearly split above 290 GHz. The highest spectral resolution $h/w = 8.59 \pm 0.53$ was achieved at 685 GHz. Above 836 GHz, we observed a shift of the g-factor and broadening of the absorption lines. Similar results have been reported using the transmission method under the pulsed magnetic field.[18] Zeeman splitting at a high magnetic field is no longer much smaller than the energy difference between the ground state and the first excited state. Therefore, the contribution from the excited states is not negligible and results in deviation from the simple linear relationship for paramagnetic resonance. In addition to the linewidth broadening, the lower quality of emitted THz-wave by the BWO at higher frequencies causes the irregular lineshapes and degradation of the spectral resolution. The spurious oscillation mode sometimes found close to the main frequency is particularly problematic. The difference in the phases between the photothermal and ESR-induced oscillations, which causes the inverse of the polarity of ESR signal, can also affect the lineshape. However, the frequency dependence of the two peaks is a direct evidence that the observed signals are ESR absorption.

The minimum detectable spin number is estimated to be $(1.4 \pm 0.2) \times 10^{15}$ spins with a S/N of approximately 5 above 1 THz. This value corresponds to the spin sensitivity of $(1.1 \pm 0.5) \times 10^{12}$ spins/G. Sensitivity is further improved by increasing the power density of THz-wave in the sample space. The experimental setup in this study used the concentrating horn, whose cutoff frequency is around 80 GHz to cover the broad frequency range. Since the 300 μm wavelength at 1 THz is comparable to sample dimensions, a significant improvement is expected through the horn design optimization.

In conclusion, we extended the frequency region of the cantilever-detected ESR technique to the THz region. Despite the small sample mass and low power output of the BWO, we observed ESR absorption of Co Tutton salt up to 1.1 THz. We believe this technique will contribute to research using high-frequency ESR in many fields.

This study was partly supported by a Grant-in-Aid for Scientific Research (B) (No. 26287081), a Grant-in-Aid for Challenging Exploratory Research (Nos. 25610075 and 26610104), and the Canon Foundation.

[1]Bruker Biospin Corporation, Germany.
[2]Y. Miyajima, H. Yashiro, T. Kashiwagi, M. Hagiwara, and H. Hori, J. Phys. Soc. Jpn. **73**, 280 (2004).
[3]C. P. Poole, Jr., *Electron Spin Resonance*, 2nd ed. (Dover, New York, 1996)
[4]M. Motokawa, H. Ohta, and N. Maki, Int. J. Infrared Millimeter Waves **12**, 149 (1991).
[5]E. del Barco, A. D. Kent, E. C. Yang, and D. N. Hendrickson, Phys. Rev. Lett. **93**, 157202 (2004).
[6]B. Cage, S. E. Russek, D. Zipse, and N. S. Dalal, J. Appl. Phys. **97**, 10M507 (2005).
[7]T. Sakurai, R. Goto, N. Takahashi, S. Okubo, and H. Ohta, J. Phys.: Conf. Ser. **334**, 012058 (2011).
[8]T. Sakurai, K. Fujimoto, R. Goto, S. Okubo, H. Ohta, and Y. Uwatoko, J. Magn. Res. **223**, 41 (2012).
[9]E. Ohmichi, N. Mizuno, M. Kimata, and H. Ohta, Rev. Sci. Instrum. **79**, 103903 (2008).
[10]D. Rugar, C. S. Yannoni, and J. A. Sidles, Nature **360**, 563 (1992).
[11]F. Hallak, J. van Slageren, and M. Dressel, Rev. Sci. Instrum. **81**, 095105 (2010).
[12]E. Ohmichi, S. Hirano, and H. Ohta, J. Magn. Reson. **227**, 9 (2013).
[13]E. Ohmichi, N. Mizuno, M. Kimata, H. Ohta, and T. Osada, Rev. Sci. Instrum. **80**, 013904 (2009).
[14]S. Kuehn, S. A. Hickman, and J. A. Marohn, J. Chem. Phys. **128**, 052208 (2008).
[15]Y. Tokuda, S. HIrano, E. Ohmichi, and H. Ohta, J. Phys.: Conf. Ser. **400**, 032103 (2012).
[16]E. Ohmichi and T. Osada, Rev. Sci. Instrum. **73**, 3022 (2002).
[17]A. McCollam, P. G. van Rhee, J. Rook, E. Kampert, U. Zeitler, and J. C. Maan, Rev. Sci. Instrum. **82**, 053909 (2011).
[18]S. Kuroda, M. Motokawa, and M. Date, J. Phys. Soc. Jpn. **44**, 1797 (1978).